Cell Death and Differentiation (2004) 11, 842–852

www.nature.com/cdd

Selectivity of protein carbonylation in the apoptotic response to oxidative stress associated with photodynamic therapy: a cell biochemical and proteomic investigation

B Magi[1,4], A Ettorre[1,4], S Liberatori[1], L Bini[1], M Andreassi[2], S Frosali[3], P Neri[1], V Pallini[1] and A Di Stefano*[,1]

[1] Department of Molecular Biology, University of Siena, via Fiorentina 1, Siena 53100, Italy;
[2] Department of Pharmaceutical Science and Technology, University of Siena, via A. Moro, S. Miniato, Siena 53100, Italy;
[3] Department of Neuroscience, University of Siena, via A. Moro, S. Miniato, Siena 53100, Italy
[4] Both these authors contributed equally to this work.
* Corresponding author: A Di Stefano, Department of Molecular Biology, University of Siena, via Fiorentina 1, 53100 Siena, Italy. Tel: +39-0577-234906; fax: +39-0577-234903; E-mail: distefano@unisi.it

Received 17.12.03; accepted 29.1.04; published online 16.4.04
Edited by V De Laurenzi

Abstract

We previously reported that photodynamic therapy (PDT) using Purpurin-18 (Pu-18) induces apoptosis in HL60 cells. Using flow cytometry, two-dimensional electrophoresis coupled with immunodetection of carbonylated proteins and mass spectrometry, we now show that PDT-induced apoptosis is associated with increased reactive oxygen species generation, glutathione depletion, changes in mitochondrial transmembrane potential, simultaneous downregulation of mitofilin and carbonylation of specific proteins: glucose-regulated protein-78, heat-shock protein 60, heat-shock protein cognate 71, phosphate disulphide isomerase, calreticulin, β-actin, tubulin-α-1-chain and enolase-α. Interestingly, all carbonylated proteins except calreticulin and enolase-α showed a pI shift in the proteome maps. Our results suggest that PDT with Pu-18 perturbs the normal redox balance and shifts HL60 cells into a state of oxidative stress, which systematically induces the carbonylation of specific chaperones. As these proteins normally produce a prosurvival signal during oxidative stress, we hypothesize that their carbonylation represents a signalling mechanism for apoptosis induced by PDT.

Cell Death and Differentiation (2004) **11,** 842–852.
doi:10.1038/sj.cdd.4401427
Published online 16 April 2004

Keywords: apoptosis; flow cytometric analysis; proteomic analysis; PDT; protein carbonylation

Abbreviations: anti-DNP, anti-2,4dinitrophenol antibody; CHAPS, 3-[(3-cholamidopropyl)dimethyl-ammonio]-1-propanesulphonate; 2-D, two-dimensional gel electrophoresis; DCFH-DA, 2′,7′-dichlorofluorescein diacetate; DMSO, dimethylsulphoxide; DNPH, 2,4-dinitrophenylhydrazine; $\Delta\psi_m$, Mitochondrial Transmembrane Potential; DTE, dithioerythritol; DTT, dithiothreitol; FACS, fluorescence-activated cell sorter; FCS, foetal calf serum; GSH, reduced glutathione; HEPES buffer, N-[2-hydroxyethyl]piperazine-*N*′-[2-ethanesulphonic acid]; OPT, *o*-phthaldialdehyde; PBS, phosphate-buffered saline; PDT, photodynamic therapy; PI, propidium iodide; Pu-18, Purpurin-18; Rhod123, Rhodamine123; ROS, reactive oxygen species; SDS, sodium dodecyl sulphate

Introduction

Apoptosis is an active highly conserved process that plays an important role in the development, homeostasis and maintenance of multicellular organisms. Apoptotic mechanisms participate in the removal of toxicologically or genetically damaged cells. Inappropriate apoptosis is associated with many diseases, including cancer.[1,2] Apoptosis is triggered by precise signals that induce crucial biochemical changes in target cells, including activation of caspases, mitochondrial depolarization, nucleosomal DNA fragmentation and alterations in the pattern of protein expression and stability.[3,4]

Recent evidence suggests that oxidative stress is a potential common mediator of apoptosis.[5] Many of the chemical and physical treatments capable of inducing apoptosis also evoke oxidative stress.[6] One of them is photodynamic therapy (PDT), an approved treatment for several types of cancer as well as for age-related macular degeneration.[7] It utilizes a bimodal protocol including a combination of photosensitizer and visible light. The interaction of light with photosensitizer molecules in the presence of molecular oxygen catalyses the formation of reactive oxygen species (ROS) within cells to produce the cytotoxic effect.[8,9] Apoptotic and necrotic pathways are both involved in cell death after PDT.[10–12] In cell culture, the oxidative stress induced by PDT triggers a series of events, including activation of phospholipase A2 and C,[13] release of nitric oxide,[14] activation of stress kinases,[12] nuclear factor kB,[15] and increased expression of early response genes[16] and heat-shock proteins (HSP's).[17] It has been reported that the apoptotic response depends on the nature of the photosensitizer, the subcellular localization of the sensitizer, the cell types used and the treatment conditions.[12] However, the critical events and specific targets triggering apoptosis after PDT remain to be investigated.

Recent studies support the concept that oxidative damage to proteins during oxidative stress and ageing is selective, and that proteins with specific sensitivity to oxidation can regulate cellular signalling events, including apoptosis.[18–22] Therefore, we hypothesized that oxidative stress associated with PDT

induces selective oxidation of specific target proteins, which could play a key role in the induction of apoptosis. The most widely studied oxidative stress-induced modification of proteins is the formation of carbonyl groups in some amino-acid side chains.[23] Oxidized proteins can be detected by Western blotting because the protein-bound carbonyl groups react with 2,4-dinitrophenylhydrazine (DNPH) and can be recognized by anti-2,4-dinitrophenol antibodies (anti-DNP).[24] To test our hypothesis, we used cytofluorimetric analysis of dying cells, two-dimensional gel (2-D) electrophoresis coupled with immunoblotting proteins and mass spectrometry. The major goal of this study was to identify specific carbonylated proteins and to relate their function to apoptosis.

As photosensitizer we used Purpurin-18 (Pu-18), a chlorophyll derivative and photoactive pigment. We previously reported that Pu-18 in combination with red light induces apoptosis in HL60 cells via caspase-3.[10] We were interested in evaluating Pu-18 because its anhydride group provides the possibility of coupling the photosensitizer to cell-targeting agents like antibodies. Our experiments were conducted on HL60 cells that are very sensitive to various stimuli including oxidative stress and PDT; hence, they are a good model to highlight the markers of apoptosis.

First, we used cytofluorimetric analysis of dying cells to monitor the relationships among the time course of ROS generation, mitochondrial transmembrane potential ($\Delta\psi_m$), changes in glutathione (GSH) content and the degree of apoptosis. When the cells induced to apoptosis by PDT had been characterized for critical parameters of cellular redox status and the most representative conditions of response time had been established, we proceeded with the separation of proteins in normal and treated cells by high-resolution 2-D electrophoresis, as well as the evaluation of carbonylated proteins by Western blotting with specific antibodies.

Proteome analysis combined with immunoblotting with specific antibodies (functional proteomics) is a powerful tool to study a family of proteins with the same post-translational modification such as carbonylation.

We show here that apoptosis induced by PDT with Pu-18 is associated with ROS generation, changes in $\Delta\psi_m$ and GSH depletion. For the first time, we demonstrate the specific oxidation of a set of proteins in HL60 dying by PDT-induced apoptosis; these proteins include molecular chaperones, such as glucose-regulated protein-78 (Grp78), Hsp60, heat-shock protein cognate 71 (Hsc71), phosphate disulphide isomerase (PDI) and calreticulin, as well as other proteins such as β-actin, tubulin-α-1-chain and enolase-α. The peculiar function of the most oxidized proteins supports the idea that protein oxidation is a signalling mechanism for apoptosis induced by PDT.

Results

PDT with Pu-18 induces ROS generation, depletion of cellular GSH, changes in $\Delta\psi_m$ and apoptosis

We reported previously that Pu-18 at nanomolar concentrations in combination with red light (1 J/cm^2) induced rapid apoptotic cell death, as documented by subdiploid DNA content and phosphatidylserine (PS) exposure in the human leukaemia cell line (HL60) via caspase-3. The present studies were undertaken to further characterize these initial results.

In the first series of experiments, we evaluated the time course of ROS generation, GSH content and mitochondrial changes; these are critical parameters of the redox status of cells and are important for the investigation of oxidized proteins. We monitored the intracellular ROS formation in HL60 cells after PDT with Pu-18 by measuring the conversion of nonfluorescent 2′,7′-dichlorofluorescein diacetate (DCFH-DA) to fluorescent DCF by flow cytometry. Preliminary experiments showed that it was possible to evaluate the time course of ROS production with adequate precision if the cells were preincubated with DCFH-DA 30 min before irradiation (to evaluate ROS production within 1 h after PDT) or at appropriate time points during the last 30 min before cell harvesting (for ROS production 2–4 h after PDT). Figure 1a shows an intense generation of ROS in HL60 cells incubated for 16 h with Pu-18 and then exposed to red light (1 J/cm^2). The ROS generation proceeded in two phases: the first increase was recorded 15 min after PDT, with maximal levels at 1 h and a decrease after 2 h; the second increase occurred at 4 h after treatment.

GSH, an intracellular antioxidant defence, is the principal detoxifying system capable of scavenging ROS and maintaining the redox state of cellular thiols. Hence, ROS generation may lead to the depletion of GSH. Therefore, we used flow cytometry to measure the single-cell o-phtaldialdehyde (OPT) fluorescence in order to examine whether PDT with Pu-18 changes the GSH content. A large percentage of untreated cells had high levels of glutathione, whereas a small percentage had low GSH content; the latter population increased in number after PDT and after 4 h about 90% of all cells showed a decrease in intracellular GSH levels, indicating that PDT induces GSH depletion (Figure 1b).

We then used flow cytometry to evaluate if PDT with Pu-18 induces changes in $\Delta\psi_m$, as shown by decreased fluorescence of Rhodamine 123 (Rhod123), a lipophilic cationic probe that becomes localized in the mitochondria of viable cells because of the relatively high electric potential across the mitochondrial inner membrane. Figure 1c illustrates the time course of changes in $\Delta\psi_m$ after irradiation. Control cells display a baseline level of fluorescence representing normal transmembrane potential. Early on (0–15 min), a subpopulation of cells gained green fluorescence (consistent with a higher $\Delta\psi_m$), while at different times after PDT the proportion of cells with reduced $\Delta\psi_m$ increased in a time-dependent manner and remained high until 4 h after irradiation.

To correlate these biochemical parameters with apoptosis, we also report the degree of apoptosis at the same times, evaluated as the amount of subdiploid DNA (Figure 1d). The increase in the sub-G0/G1 peak at different times after PDT is correlated with the drop in $\Delta\psi_m$. Analysis of the percentage of cells in the different cell cycle phases (by MODFIT) revealed no significant change at any time (data not shown). Light alone or Pu-18 in the absence of light did not induce changes in the biochemical parameters.

2-D reference map of HL60 cells

To identify particular changes associated with apoptosis induced by PDT with Pu-18, we separated the proteins in normal and treated cells by high-resolution 2-D electrophoresis. We

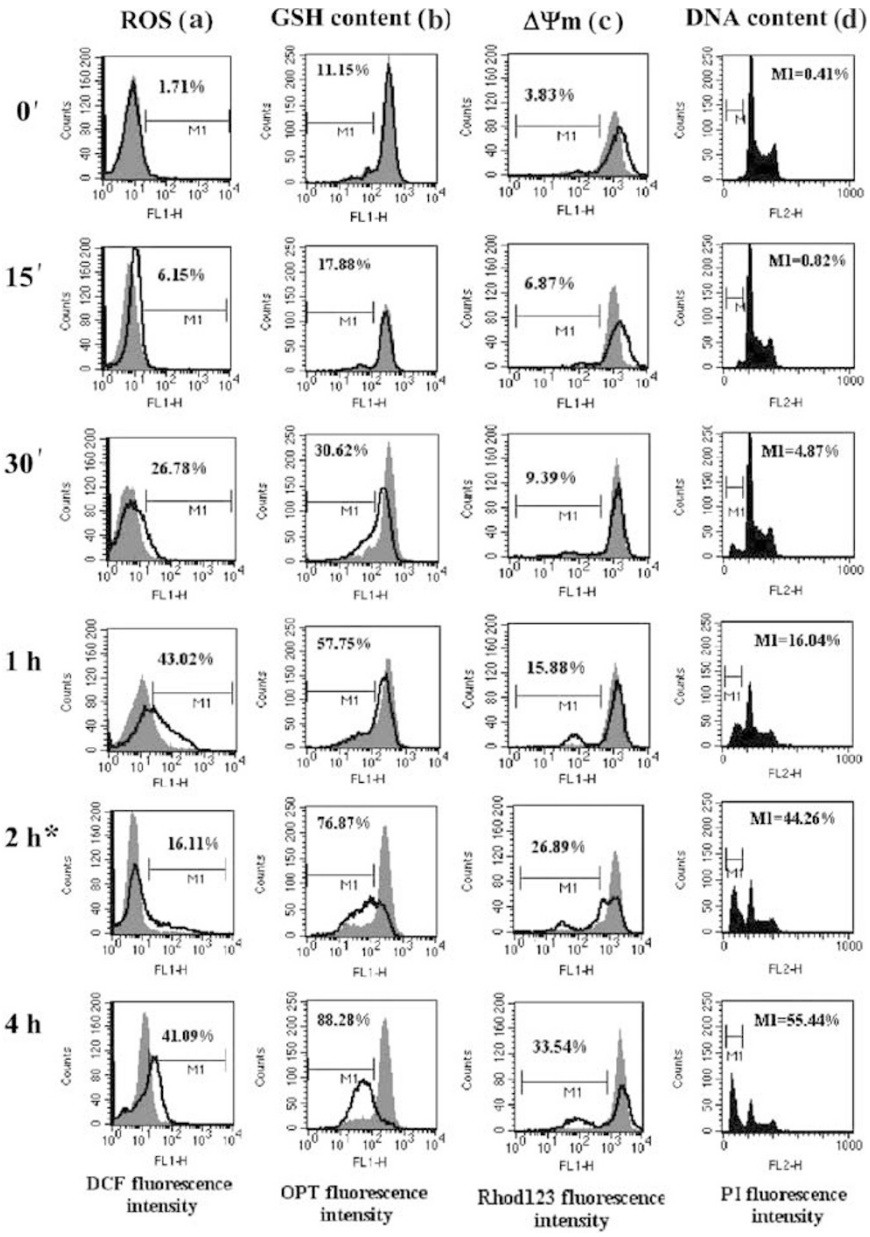

Figure 1 Flow cytometric analysis of the time course of ROS generation, GSH content, $\Delta\psi_m$ and cell cycle profiles after PDT with Pu-18. Cells were treated with 0.5 μM Pu-18 for 16 h and exposed to a light dose of 1 J/cm^2. At the indicated times after irradiation, cells were collected and the different assays were performed as described in 'Materials and Methods'. The number of cells is indicated on the *Y*-axis. Filled histograms correspond to control cells while open histograms represent PDT-treated cells. The logarithm of fluorescence intensity in the FL1-H channel (*X*-axis) is an indicator of ROS production (**a**), changes in GSH content (**b**) and changes in $\Delta\psi_m$ (**c**), while the fluorescence intensity in the FL2-H channel (*X*-axis) reflects DNA content. The figure is representative of four different experiments. (*) indicates the cells used for 2-D electrophoresis and immunoblotting

considered 2 h after PDT an appropriate time to perform proteome analysis, since at this time the production of ROS was declining, most cells (75%) showed a GSH depletion and about 45% of them were apoptotic. The protein pattern of HL60 cells obtained by 2-D PAGE is shown in Figure 2. With 60 μg of total protein lysate, more than 1000 spots were resolved on silver-stained gels in the pI range from 3 to 10 and the molecular mass range from 10 to 250 kDa. We identified several spots, including Grp78, Hsc71, PDI, Hsp60, β-actin, Grp75, PDI-ER60 and triosephosphate isomerase, by matching them with HL60 cell reference maps available through the Swiss 2-D PAGE database (http://www.expasy.org).

MALDI-TOF mass spectrometry confirmed the assignments based on gel matching and allowed the identification, for the first time, of other spots corresponding to seven proteins (Figure 2, Table 1): mitofilin, KH-type splicing regulatory protein, pyruvate kinase, enolase-α, phosphoglycerate kinase, fructose-biphosphate aldolase A, tubulin-α-1-chain. Figure 3 shows a typical peptide mass fingerprint

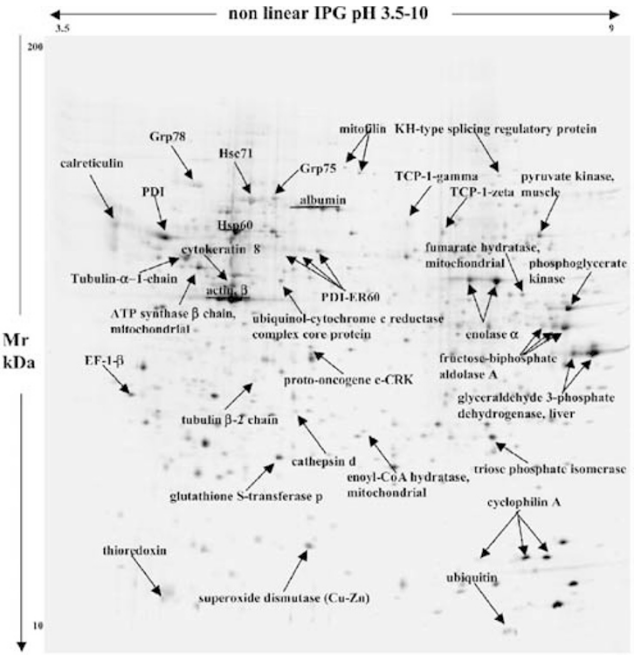

Figure 2 2-D electrophoretic pattern of HL60 cells, obtained using a non-linear Immobiline pH gradient 3–10 followed by 9–16% SDS-PAGE. Proteins (60 μg) were detected by silver staining. Whole-cell extracts from HL60 cells were prepared as described in 'Materials and Methods'. Proteins are indicated in Table 1

spectrum obtained from the 2-D separated spot corresponding to mitofilin.

Differential analysis by 2-D gel electrophoresis

Computer analysis performed with Melanie 3 showed that PDT with Pu-18 induced only very limited qualitative and quantitative changes in the protein pattern of HL60 lysates obtained at 2 h after treatment (Figure 4a and b). We repeated the same experiment four times; only the changes observed in all the experiments, and only when the spots changed by almost three times their volume, were considered significant. No changes in protein pattern occurred when the treatment with Pu-18 occurred in the dark (data not shown). At 2 h after irradiation, only 19 of more than 1000 protein spots resolved were found to be modified during PDT-induced apoptosis: the expression of at least two proteins, mitofilin and spot 6, decreased; two unidentified proteins appeared increased (spots 4–5) and four emerged (spots 7–10) during apoptosis (Figure 4; Table 2).

The most striking feature of the proteome maps of apoptotic cells is the appearance of additional or increased amounts of acidic isoforms of nine proteins: Grp78, Hsc71, PDI, Hsp60, β-actin, tubulin-α-1-chain (the identity of these proteins was confirmed by mass spectrometry) plus other unidentified proteins (indicated by numbers 1–2–3) (Figure 4; Table 2). This suggests that post-translational modifications occurred in the apoptotic cells. We then investigated if the appearance of acidic isoforms also occurred after a classical model of apoptosis-inducing oxidative stress, i.e. treatment with hydrogen peroxide (H_2O_2) at a final concentration 150 μM for 4 h. The acidic spots did not appear in these conditions (data not shown), suggesting that the particular pattern is associated with PDT. When we used necrosis-inducing doses of PDT, massive cell death occurred after only 1 h and the accompanying cell lysis (documented by loss of proteins) precluded a correct 2-D analysis (data not shown).

Table 1 List of proteins identified by gel matching and mass spectrometry

Protein	Accession no.	Identification method
Calreticulin	P 27797	GM-MS
Grp 78	P 11021	GM-MS
Heat shock cognate 71 a protein	P 11142	GM-MS
Mitofilin	Q16891	MS
KH-type splicing regulatory protein		MS
PDI	P07237	GM-MS
Hsp60	P10809	GM-MS
Grp75	P38646	GM-MS
Albumin	P02768	GM
Cytokeratin 8	P05787	GM
TCP-1-gamma	P49368	GM
TCP-1-zeta	P40227	GM
Pyruvate kinase, muscle	P14618	MS
Fumarate hydratase, mitochondrial	P07954	GM
Phosphoglycerate kinase	P00558	MS
Tubulin-α-1-chain	P05209	MS
PDI-ER 60	P30101	GM-MS
β-actin	P02570	GM-MS
ATP synthase beta chain, mitochondrial	P06576	GM- MS
Ubiquinol–cytochrome *c* reductase complex core protein	P31930	GM-MS
Enolase alpha	P06733	MS
Fructose-biphosphate aldolase a	P04075	MS-MS
EF-1-beta	P24534	GM
Proto-oncogene c-CRK	P46108	GM
Tubulin-β-2-chain	P05217	GM
Glyceraldehyde-3-phosphate dehydrogenase, liver	P04406	GM
Cathepsin d	P07339	GM
Glutathione s-transferase p	P09211	GM
Enoyl-CoA hydratase, mitochondrial	P30084	GM
Triose phosphate isomerase	P00938	GM-MS
Ciclophylin A	P05092	GM-MS
Thioredoxin	P10599	GM
Superoxide dismutase (Cu–Zn)	P00441	GM
Ubiquitin	P02248	GM

GM = gel matching; MS = mass spectrometry

PDT with Pu-18 induces carbonylation of specific proteins

To evaluate the oxidized proteins after PDT, we used 2-D electrophoresis combined with immunoblotting with specific antibodies. Oxidized proteins can be detected by Western blotting because the protein-bound carbonyl groups react with DNPH and can be recognized by anti-DNP antibodies. Analysis of the oxidized proteins revealed that the oxidation was not random but specific and occurred systematically 2 h after PDT in four experiments. Typical results are shown in Figure 5a and b. In comparison with control cells, there is an evident increase in the number of carbonylated spots appearing in a relatively small area of the immunostained

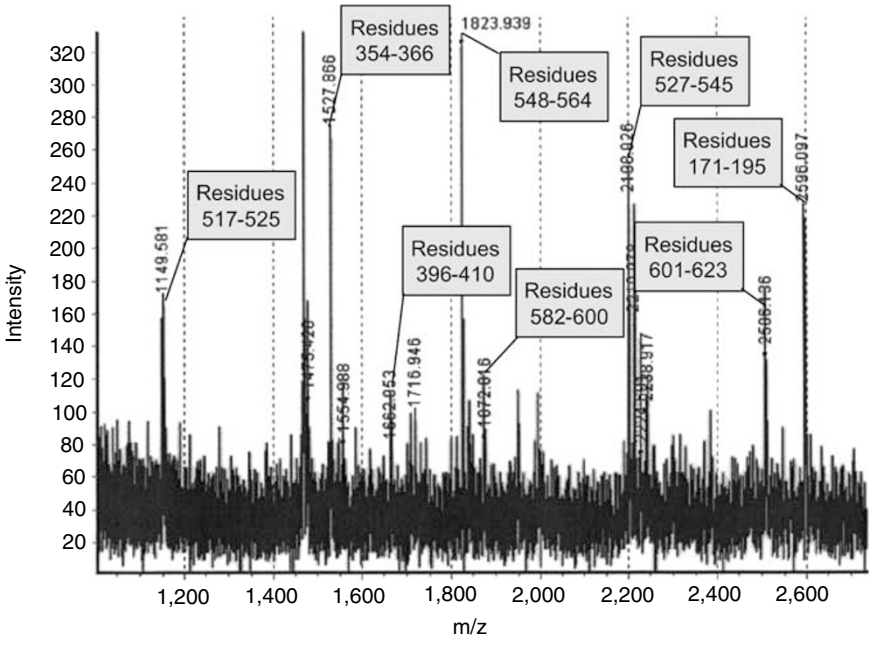

Figure 3 Peptide mass fingerprinting spectrum of mitofilin (mitochondrial inner membrane protein Q16891) obtained with an Ettan MALDI-ToF Pro as described in 'Materials and Methods'

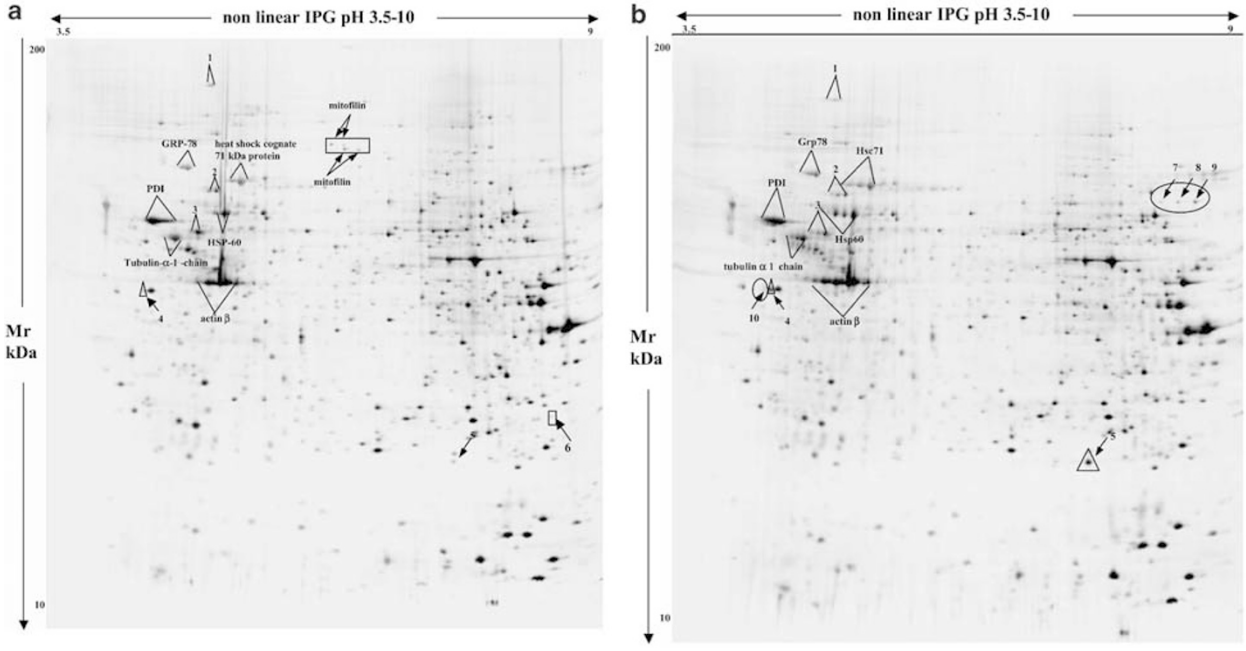

Figure 4 Differences in protein patterns from control HL60 cells (**a**) and Pu-18-treated HL60 cells (**b**). Proteins not yet identified are indicated by numbers. Whole-cell extracts from HL60 cells obtained 2 h after PDT with Pu-18 were prepared as described in 'Materials and Methods'. Arrows: protein spots with changes of almost three times the volume in all experiments; Circles: spots emerging in apoptotic cells; Squares: spots disappearing in apoptotic cells; Triangles: spots displaying increasing intensity in apoptotic cells; Convergent Arrows: spots with a pI shift. We repeated the same experiment four times and the figure represents a typical experiment

gel, ranging from M_r 78 KD to 41 kDa and from pH 4.3 to 6.7. A slight degree of carbonylation, which increased after PDT, occurred in control cells only for tubulin-α-1-chain, but this is not surprising since the generation of ROS occurs only in physiological conditions. We detected another seven carbonylated proteins in treated cells: β-actin, Hsc71, Grp78, Hsp60, PDI, calreticulin and enolase-α and the unidentified spot 3. Interestingly, seven of the carbonylated proteins (Grp78, Hsc71, Hsp60, PDI, tubulin-α-1-chain, β-actin and spot 3) also showed the pI shift, while the other two, calreticulin and enolase-α, lacked an isoelectric shift (Table 2).

Table 2 (a) Protein alterations with respect to control in apoptotic cells 2 h after PDT with Pu-18 and (b) Frequency of modifications among 19 modified spots in apoptotic cells 2 h after PDT with Pu-18

	Quantitative Differences				
Protein	Control	Pu-18 treated	Isoelectric shift	Carbonyl groups	
(a)					
1	=	=	Yes	No	
Mitofilin	+	−	No	No	
Grp78	=	=	Yes	Yes	
Hsc71	=	=	Yes	Yes	
2	=	=	Yes	No	
Calreticulin	=	=	No	Yes	
PDI	=	=	Yes	Yes	
Hsp60	=	=	Yes	Yes	
3	=	=	Yes	Yes	
Tubulin-α-1-chain	=	=	Yes	Yes↑	
Enolase-α	=	=	No	Yes	
β-actin	=	=	Yes	Yes	
4	+	++	No	No	
5	+	++	No	No	
6	+	−	No	No	
7	−	+	No	No	
8	−	+	No	No	
9	−	+	No	No	
10	−	+	No	No	
Decrease	Increase	Isoelectric shift	Carbonylated	Isoelectric shift with Carbonylation[a]	Carbonylation without Isoelectric shift
(b)					
2/19	6/19	9/19	9/19	7/19	2/19

[a]These seven proteins are indicated in bold in (a). +, spot present; ++, increased intensity; =, intensity not significantly changed; −, spot absent; ↑, increased intensity of carbonylation compared to control

Discussion

In a previous study, we demonstrated that HL60 cells treated with Pu-18 and light exhibited DNA laddering, activation of caspase-3 and an increase in subdiploid DNA and phosphatidylserine externalization, indicating DNA fragmentation and loss of membrane phospholipid asymmetry. The PS exposure and the nuclear features of apoptosis were prevented by the treatment of the cells before illumination with the caspase inhibitors, benzyloxycarbonyl-Val-Ala-Asp-fluoromethylketone (z-VAD-FMK) and benzyloxycarbonyl-Asp-Glu-Val-Asp- fluoromethylketone (z-DEVD-FMK).[10]

In this study, we have shown that several inter-related events occur in HL60 cells during apoptosis induced by PDT with Pu-18. In the first experiments, the time course (0–4 h) of ROS generation, glutathione content, mitochondrial changes and apoptosis were monitored by flow cytometry. We showed that apoptosis induced by PDT with Pu-18 was preceded by a transient hyperpolarization of $\Delta\psi_m$, an increase of ROS generation and GSH depletion. These events were followed by disruption of $\Delta\psi_m$ and cell death. The time course of ROS generation showed that PDT increased the level of ROS, with two peaks at 1 and 4 h. It has been reported that PDT produces singlet oxygen[8,12] and DCF does not detect $O_2^{\cdot}$, but rather reacts with hydroperoxides. Therefore, the initial increase of ROS generation is likely due to the reactivity of $O_2^{\cdot}$ formed early after PDT and its ability to induce the formation of other ROS species that can be detected by DCF. The late increase of ROS production, detected 4 h after PDT, is likely a downstream event associated with the drop in $\Delta\psi_m$.

The early transient increase of $\Delta\psi_m$ is consistent with recent studies showing an early increase of $\Delta\psi_m$ followed by a drop in $\Delta\psi_m$ as a late event in apoptosis.[25,26]

ROS generation in the first hour after PDT was correlated with GSH depletion. At later times after PDT, the percentage of cells with glutathione depletion increased dramatically until 4 h when most cells were GSH depleted. Flow cytometric analysis of DNA content showed that apoptotic cell death rapidly increased beginning at 1 h after PDT and was nearly complete after 6 h, as reported previously.[10] The drop in $\Delta\psi_m$ was simultaneous with the increase of the sub-G0/G1 peak and occurred over a similar time course, even though it appeared to be restricted to a smaller number of cells. The time-course studies suggested that the high levels of ROS, associated with reduced GSH content and mitochondrial changes, can perturb the normal redox balance and shift HL60 cells into a state of oxidative stress that induces apoptosis. Our results are consistent with recent reports showing that the changes in cellular redox potential due to enhanced ROS generation and depletion of reduced glutathione are sufficient to induce the opening of mitochondrial megachannels, leading to the disruption of the $\Delta\psi_m$ and finally the release of cell death-promoting factors, including cytochrome *c* and apoptosis-inducing factor (AIF).[27,28] Moreover, the loss of $\Delta\psi_m$ is an apoptotic event reported for several photosensitizers whose principal site of localization is the mitochondrion,[9,29] such as Pu-18.[30]

To define the role of changes in HL60 redox status after PDT from another point of view, we recorded protein changes and oxidation using the proteomics approach, which is

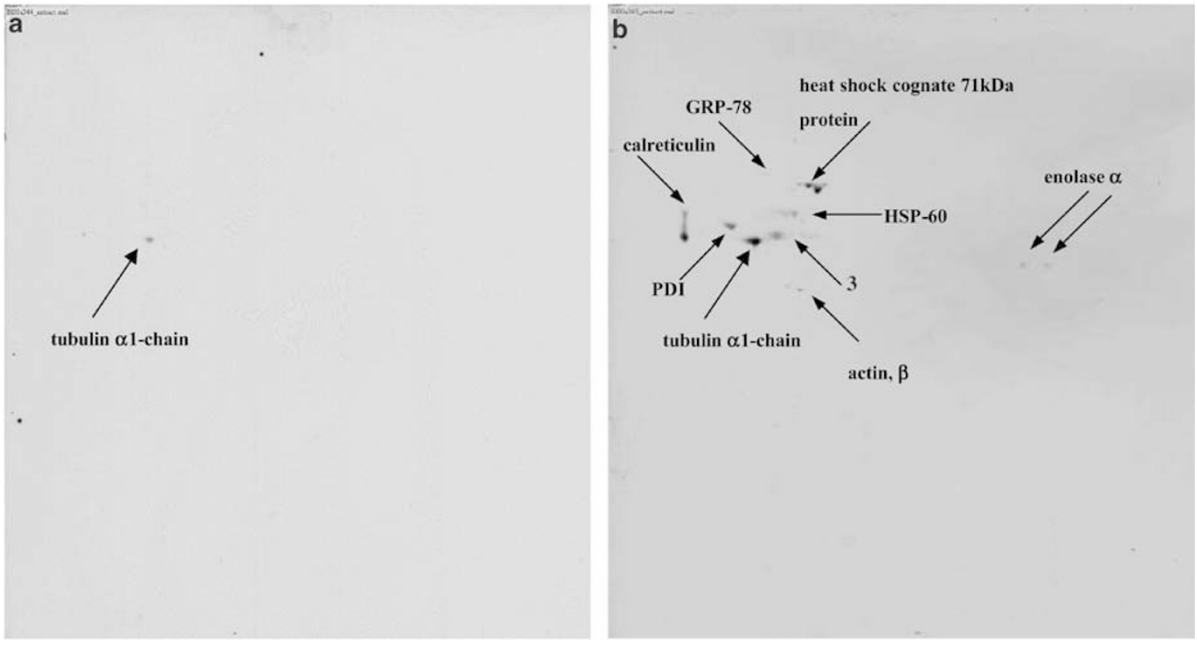

Figure 5 Immunostaining with an anti-DNP antibody of proteins from control HL60 cells (**a**) and Pu-18-treated HL60 cells (**b**), separated by 2-D electrophoresis and derivatized by DNPH as described in 'Materials and Methods'. The immunoblotting for control and treated cells corresponds to the 2-D maps reported in Figure 4. The arrows indicate the carbonylated proteins. We repeated the same experiment four times and the figure represents a typical experiment

particularly suited to studies of the integrated cellular response to oxidative stress, for example, during PDT. The proteome analysis was performed at 2 h after PDT when the production of ROS was declining, most cells (75%) showed GSH depletion and about 45% of them were apoptotic. Since all cells were dead by apoptosis after 24 h as reported previously,[10] it is reasonable to suppose that all cells were committed to apoptosis at 2 h. Of the more than 1000 protein spots separated on the HL60 cell protein maps, only six unidentified spots were enhanced and two were suppressed following treatment with Pu-18. Interestingly mitofilin, a mitochondrion-associated protein, is down-regulated in apoptotic cells. Four spots related to mitofilin appeared to be decreased in HL60 undergoing PDT-induced apoptosis. Gieffers *et al*.[31] demonstrated that mitofilin is a transmembrane protein of the inner mitochondrial membrane, expressed as two isoforms and transported into the mitochondrion in a reaction that depends on the $\Delta\psi_m$.[32] As PDT with Pu-18 caused the loss of $\Delta\psi_m$ and the function of this ubiquitous mitochondrial protein is currently unknown, it is tempting to speculate that mitofilin plays a role in apoptosis induced by PDT with Pu-18.

After a detailed look at the maps of apoptotic cells, the most striking aspect was the appearance of acidic isoforms of structural proteins (β-actin, tubulin-α-1-chain), several proteins with chaperone functions (Grp78, Hsp60, Hsc71, PDI) and unidentified proteins (spots 1, 2 and 3), possibly reflecting selective post-translational modifications. It is interesting that a proteome analysis by Gerner *et al*.[33] demonstrated that two protein families, cytoskeletal proteins (like β-actin) and chaperone proteins, were predominantly affected in Fas-induced apoptosis. Moreover, Grebenova *et al*.[34] reported that three ER chaperones involved in calcium homeostasis (calreticulin, PDI and ERp57) were downregulated in HL60 cells treated with ALA-PDT. The increase of acidic isoforms of some proteins seems to be peculiar to PDT. When we used mild doses of H_2O_2 as a source of ROS, there was no increase of acidic isoforms of specific proteins, while Raggiaschi *et al*.[35] reported an extension towards the acidic side of some proteins in *Candida albicans* after PDT with cationic tetra-substituted phthalocyanines. The most widely studied oxidative stress-induced modification of proteins is the formation of carbonyl groups, which can occur by different mechanisms, including direct oxidation of side chains of lysine, arginine, proline and threonine residues. The analysis of stress-induced carbonylated proteins is very interesting because the carbonylation is increased after oxidative stress and is involved in the etiology and progression of many human pathologies, such as cancer, rheumatoid arthritis and pulmonary disease, as well as other physiological conditions such as ageing and inflammation.[18,36,37] Several studies have also shown increases in protein carbonyls in Alzheimer's[38] and Parkinson's diseases.[39] Using 2-D electrophoresis combined with immunoblotting with anti-DNP, we demonstrated that only a few proteins were particularly sensitive to oxidative stress. Interestingly, the carbonylated proteins were the same ones that showed the pI shift, plus calreticulin and α-enolase. The presence of carbonylated mitochondrial, cytosolic and endoplasmic reticulum (ER) proteins support the idea of a generalized intracellular state of oxidative stress after PDT, and suggests that only certain proteins are the targets of PDT-generated ROS. It is evident that the degree of carbonylation was not correlated to the amount of proteins: in fact, some proteins that appeared carbonylated were not among the largest spots. The finding that specific proteins become carbonylated clearly demonstrates that protein

carbonylation is selective, confirming our hypothesis. The specific oxidation of β-actin and tubulin-α-1-chain in association with oxidative stress has been reported in the brain of Alzheimer patients.[38] Oxidation of β-actin during oxidative stress may affect actin filament architecture and lead to disorganization of the cytoskeleton to form apoptotic blebs typical of apoptosis.

The specific oxidation of Hsp's is interesting and very exciting. The HSP's also known as molecular chaperones, help guide protein transport and folding under physiological conditions; they also prevent aggregation and aberrant folding during stress and are involved in the immune response.[40] Their expression increases the survival of cells exposed to numerous types of stimuli that lead to apoptosis, including oxidative stress, treatment with apoptosis-inducing agents and PDT.[17] In humans, the HSP70 multigene family consists of four members with high homology: Hsc70, Hsp70, Grp78 and Hsp75.[41] HSP70 multigene family proteins play a role in protein assembly, but the level of single chaperone proteins in response to stress can vary. Hsp70.1 is highly stress - induced, while Hsc71 is the constitutive isoform, recruited by the cell as a primary defence against unfavourable conditions.[41]

Hsp60 is a mitochondrial chaperone and its overexpression protects mitochondrial function and prevents apoptosis induced by ischaemia.[42] Calreticulin is one of the major calcium-binding proteins in the lumen of the ER.[43] Several of these proteins negatively interfere with apoptosis: in particular, Hsp70 protects against apoptosis by inhibiting caspase cascade activation and can inhibit apoptosis by neutralizing and interacting with AIF, a mitochondrial flavoprotein that translocates to the nucleus via the cytosol after the induction of apoptosis.[41,44,45] The induction of HSP's is a well-known response to PDT, but the cellular heat-shock response after PDT can vary significantly among different photosensitizers, cell types and treatment conditions.[16,17]

That oxidation of particular chaperones is an important event during oxidative stress is supported by the most recent literature, showing the specific oxidation of different chaperones depending on the particular stress condition: ER chaperones (PDI, Bip, calreticulin) in aged mouse liver,[46] hsc71 in the Alzheimer brain,[47] Hsp60 and vimentin in neuronal cells exposed to mild oxidative stress.[22] Moreover, molecular chaperones, such as Hsp60 in *Saccharomyces cerevisiae* and DnaK in *Escherichia coli*, were previously detected as major targets during oxidative stress, and it was suggested that these chaperones act as shields protecting proteins against oxidative damage.[19,20]

Why are chaperones particularly sensitive to oxidative stress, including PDT? Does their particular function make them susceptible to oxidative stress? It is now thought that molecular chaperones closely interact with misfolded or damaged proteins, producing effects that can be likened to 'protein massage'. An intriguing hypothesis to explain our results is that when the chaperones interact with damaged protein targets to assist their refolding, a protein–protein radical transfer can occur from oxidized proteins to chaperones. This leads to the idea that certain chaperones trying to reduce the toxic effect of oxidative stress were themselves oxidized. As protein oxidation often results in the loss of protein function, the oxidation of Hsp proteins may counteract their protective effect against oxidative stress and could provide a signal capable of triggering the suicide mechanism. Moreover, the chaperones could function as sentinels to recognize the amount of cellular damage and the extent of their oxidation could provide a pivotal decisional checkpoint to determine the cell's fate after oxidative stress. Hence, their carbonylation could result from their particular function. We suggest here that the specific carbonylation of some chaperones and their consequent inactivation could be the mechanism by which PDT kills otherwise resistant tumour cells.

The specific oxidation of β-actin, enolase-α and tubulin-α-1-chain in addition to that of chaperones suggests that the selective damage could be a consequence of the proteins' structural relationship in addition to their function. Thus, the susceptibility to oxidative stress could depend on the structure of the proteins (the particular sequence motifs, linked sugars or bound metal atoms). Only a few of the carbonylated proteins are glycoproteins and only two (Grp78 and calreticulin) have sites to bind calcium.[48] The specific oxidation of enolase-α, the only glycolytic pathway enzyme to be carbonylated, could be related to the structure of this protein. The specific sensitivity of enolase-α has been reported by others in different conditions of oxidative stress.[19,47]

A link between these two families of proteins, structural proteins and chaperones, could be their ATPase activity. All members of the Hsp70 chaperone class possess two distinct domains: a highly conserved N-terminal ATPase domain and a more different C-terminal domain. Interestingly, the N-terminal ATP domain of Hsp70 is similar to that of actin in skeletal muscle despite the low sequence similarity and the analogous positions of arginine 177 of actin and lysine 71 of Hsp, suggesting that the two proteins might utilize a similar mechanism for ATP hydrolysis.[49] This is supported by the abolition of ATPase activity by ADP -ribosylation of R177 by bacterial toxins; moreover, the lysine (K71) was found to be an essential catalytic residue for nucleotide hydrolysis by the 44-kDa N-terminal ATP domain of Hsp70. These structural relationships suggest that the carbonylation can occur on side chains of these critical residues (arginine 177 of actin and lysine 71 of Hsc71). The subsequent lack of a positive charge could be responsible for the lower pI observed on the gels for β-actin and Hsp71. We can speculate that the oxidative stress induced by PDT could lead to the addition of carbonyl groups in a residue of a particular sequence of target proteins. Further studies are in progress to identify the residues in which carbonylation occurs after PDT.

Although our protein carbonylation analysis was based on a single dose of PDT and a single time after treatment, we believe that the carbonylation of several chaperones is not only a marker of oxidative damage but could be an important event in the signalling pathway of apoptosis by PDT with Pu-18, just like specific protein phosphorylation events reported to occur during apoptosis.

In conclusion, our results indicate that oxidative stress induced by PDT evokes an orchestrated response affecting mitochondria and ER chaperones, and provide additional information on cellular targets in the apoptotic responses to oxidative stress associated with PDT.

Materials and Methods

Cell treatment

HL60 human leukaemia cells, originating from the American Type Culture Collection (Rockville, MD, USA), were kindly provided by Professor Marcella Cintorino (Istituto di Anatomia Patologica, Policlinico Le Scotte, Università degli Studi di Siena, Siena, Italy).

HL60 cells were grown in RPMI medium containing 10% foetal calf serum, 100 U/ml penicillin G and 100 μg/ml streptomycin, at 37°C in a controlled humified incubator in 5% CO_2. For the experiments, the cells at concentration of 5×10^5/ml were incubated in the dark with Pu-18 (Porphyrin Product) 0.5 μM for 16 h. After incubation, the cells were collected by centrifugation, resuspended in fresh medium at concentration of 1×10^6/ml, exposed to 1 J/cm^2 of red light and maintained in Petri dishes at 37°C until further analysis. Irradiation was carried out at room temperature with a 150 W halogen lamp using a broad spectrum 600–700 nm filter. Pu-18 was dissolved in dimethylsulphoxide (DMSO) as a 20 mM stock solution and stored at −20°C. Working solutions were prepared in culture medium immediately before use. Cells treated with vehicle (DMSO) only and light served as controls. The final DMSO concentration never exceeded 0.1%.

Flow cytometric assays

The formation of intracellular ROS was measured using 2′,7′-dichlorofluorescein diacetate (DCFH-DA, Sigma-Aldrich, Milan, Italy). By this method, it is possible to measure the amount of H_2O_2 generated by increased oxidative metabolism. Viable cells can deacetylate DCFH-DA to 2′,7′-dichlorofluorescein; the latter is not fluorescent but can react quantitatively with oxygen species within the cell to produce 2′,7′-dichlorofluorescein (DCF), which is fluorescent and is trapped inside the cell. The cytofluorimetric measurement of the DCF produced can provide an index of intracellular oxidation.[25] However, DCF can leak out of cells, making it difficult to detect H_2O_2 production at later times. Therefore, to monitor the ROS production over time, we incubated the cells with DCFH-DA (10 μM final concentration) for 30 min either before irradiation or during the last 30 min of incubation,[50] at appropriate time points after irradiation. Before analysis, 10 μl of a propidium iodide (PI, Sigma-Aldrich, Milan, Italy) stock solution (10 μg/ml final concentration) were added. For measurement of the intensity of DCF fluorescence, the cells were kept in ice until analysis with fluorescence-activated cell sorter (FACS) Calibur flow cytometer (Becton Dickinson) equipped with an excitation laser line at 488 nm and Cell Quest software (Becton Dickinson). The DCF (green fluorescence) was collected in a log scale through a 530 ± 20 band pass filter. Monoparametric histograms of the fluorescence distribution were plotted for the estimation of ROS production.

$\Delta\psi_m$ was assessed by the uptake of the cationic lipophilic dye Rhod123 and PI using a commercial product (Sigma-Aldrich, Milan, Italy) according to the method described previously.[25] Briefly, at different times after PDT, approximately 5×10^5 cells for each sample were washed twice in phosphate-buffered saline (PBS) and the pellet was resuspended in 500 μl of PBS. Rhod123 (4 μl) stock solution were added to the cell suspension (1 μg/ml final concentration) and incubated for 30 min at 37°C in the dark. Then the cells were washed in PBS and resuspended in 200 μl of binding buffer plus 10 μl of the PI stock solution (10 μg/ml final concentration). The cells, kept in ice, were analysed with a FACSCalibur. The Rhod123 (green fluorescence) and the PI (red fluorescence) were both collected in a log scale through a 530 ± 20 and 575 ± 15 nm band pass filter, respectively.

GSH content was evaluated using *o*-phthaldialdehyde (OPT) (Sigma-Aldrich, Milan, Italy) as described by Treumer and Valet.[51] Briefly, the OPT method is based on reaction with both glutathione amino- and sulphhydryl groups, yielding a cyclic highly fluorescent product. The OPT-GSH fluorescent product appears in the green fluorescence channel. For staining, 1×10^6 cells were resuspended in 500 μl HEPES N-[2-hydroxyethyl]piperazine-*N*′-[2-ethanesulphonic acid]-buffered saline pH 7.4 and OPT was added (final concentration 1 mM of a stock solution 0.1 M in dimethylformamide). After 5 min of incubation at room temperature, the suspension was immediately washed and the cells were analysed with a FACSCalibur. The OPT-GSH (green fluorescence) was collected in a log scale through a 530 ± 20 band pass filter. Monoparametric histograms of the fluorescence distribution were plotted for the estimation of GSH content.

DNA content was analysed using PI as described previously.[10] The percentages of cells in the G1, S and G2 phases were determined using the MODFIT program (Verity Software, Topahsm, ME, USA).

At least 20 000 events were collected for each sample using Cell Quest software; debris was excluded from the analysis by an appropriate morphological gate of forward scatter *versus* side scatter.

2-D electrophoresis

The HL60 cells were dissolved in lysis buffer (8 M urea, 4% CHAPS (3-[(3-cholamidopropyl)dimethylammonium]-1propanesulphonate), 40 mM Tris base, 65 mM dithioerythritol (DTE) and trace amounts of bromophenol blue). The protein concentration was determined by Biorad protein assay according to Bradford[52] and the samples were diluted in lysis buffer so that 350 μl of sample contained 60 μg of proteins.

2-D gel electrophoresis was performed essentially as described previously.[53,54] The first-dimension separation was carried out on a nonlinear wide-range immobilized pH gradient (pH 3.5-10, 18 cm long IPG strips, Amersham Biosciences). Strips were swollen in 350 μl of lysis buffer containing 60 μg of proteins and 0.8% carrier ampholytes (Resolyte pH 4–8, BDH) and a trace of bromophenol blue. The voltage was increased linearly from 300 to 3500 V during the first 3 h, then stabilized at 5000 V for 22 h (total 110 kVh). After electrophoresis, IPG strips were equilibrated for 12 min in 6 M urea, 30% w/v glycerol, 2% w/v sodium dodecyl sulphate (SDS), 0.05 M Tris-HCl, pH 6.8, 2% w/v DTE, and then for 5 min in the same urea/SDS/Tris buffer solution except that 2% DTE was replaced with 2.5% w/v iodoacetamide. For immunodetection of carbonyl groups, strips were treated after IEF with 10 mM DNPH in 5% trifluoroacetic acid and then neutralized in 0.15 M Tris pH 6.8, 8 M urea, 1% SDS, 20% glycerol, before the steps of equilibration as described.[24] The second-dimension run was carried out on 9–16% polyacrylamide linear gradient gels (18 cm × 20 cm × 1.5 mm), at 40 mA/gel constant current and 10°C, until the dye front reached the bottom of the gel. Gels were stained with ammoniacal silver nitrate as described.[55,56]

Electrophoretogram images were obtained with a computing densitometer (Molecular Dynamics 300S) and processed with Melanie 3 (GeneBio).

Immunoblotting

Proteins were electroblotted onto nitrocellulose membranes (Hybond ECL, Amersham Biosciences) using 25 mM Tris, 192 mM glycine and 20% (v/v) methanol, according to Towbin.[57] Protein transfer was carried out using a tank apparatus (trans-blot cell, BioRad) for a total of 2 Å.

Before immunodetection, the membranes were stained in 0.2% w/v Ponceau S in 3% w/v trichloroacetic acid for 3 min and the spot position

was marked to facilitate computer-assisted matching on the silver-stained gel.[58] Immunodetection was performed as described previously[58] using anti-DNP IgG (Sigma, dilution 1 : 10 000). The immunoreactive spots were detected using rabbit anti-mouse IgGs conjugated with peroxidase and a chemiluminescence detection system (Amersham Biosciences).

Protein identification of 2-D separated spots by mass spectrometry

Protein identification was carried out by MALDI-TOF and ESI-Ion Trap mass spectrometry. After visualization with Coomassie blue staining, electrophoretic spots were excised and protein digestion was carried out as described.[59,60] MS spectra were acquired using an Ettan MALDI-TOF mass spectrometer (Amersham Biosciences, Uppsala, Sweden) and peptide sequencing was carried out using an LCQ DECA ion trap mass spectrometer (Finnigan, San Jose, CA, USA). Mass fingerprinting and MS/MS database searching were carried out using ProFound (www.proteometrics.com) and Mascot (Matrix Science Ltd., London, UK, http://www.matrixscience.com) on-line-available software and TurboSEQUEST software (Finnigan, San Jose, CA, USA).

Database searching criteria were limited by the following parameters: less than 150 ppm Δmass between experimental and theoretical peptide masses, more than 20% of protein sequence coverage required and *Z*-score higher than 1.66.

Acknowledgements

We thank Mr Leonardo Taurisano for excellent technical assistance, Dr Simona Tavarini and Dr Sandra Nuti for helpful discussion with regard to the cytofluorimetric analysis and Dr Peter Christie for the careful English revision. This research was supported in part by grants from the European Commission (QLK3-CT-2001-01495) and the Piano di Ateneo per la Ricerca of University of Siena.

References

1. Thompson C (1995) Apoptosis in pathogenesis and treatment of disease. Science 267: 1456–1461
2. Kiechle FL and Zhang X (2002) Apoptosis: biochemical aspects and clinical implications. Clin. Chim. Acta 326: 27–45
3. Thornberry NA (1998) Caspases: key mediators of apoptosis. Chem. Biol. 5: R97–103
4. Hengartner MO (2000) The biochemistry of apoptosis. Nature 407: 770–776
5. Colussi C, Albertini MC, Coppola S, Rovidati S, Galli F and Ghibelli L (2000) H_2O_2-induced block of glycolysis as an active ADP-ribosylation reaction protecting cells from apoptosis. FASEB J. 14: 2266–2276
6. Chandra J, Samali A and Orrenius S (2000) Triggering and modulation of apoptosis by oxidative stress. Free Radic. Biol. Med. 29: 323–333
7. Dougherty TJ (2002) An update on photodynamic therapy applications. J. Clin. Laser Med. Surg. 20: 3–7
8. Ahmad N and Mukhtar H (2000) Mechanism of photodynamic therapy-induced cell death. Methods Enzymol. 319: 342–358
9. Lam M, Oleinick NL and Nieminen AL (2001) Photodynamic therapy-induced apoptosis in epidermoid carcinoma cells. Reactive oxygen species and mitochondrial inner membrane permeabilization. J. Biol. Chem. 276: 47379–47386
10. Di Stefano A, Ettorre A, Sbrana S, Giovane C and Neri P (2001) Purpurin-18 in combination with light leads to apoptosis or necrosis in HL60 leukemia cells. Photochem. Photobiol. 73: 290–296
11. Fabris C, Valduga G, Miotto G, Borsetto L, Jori G, Garbisa S and Reddi L (2001) Photosensitization with zinc (II) phthalocyanine as a switch in the decision between apoptosis and necrosis. Cancer Res. 61: 7495–7500
12. Oleinick NL, Morris RL and Belichenko I (2002) The role of apoptosis in response to photodynamic therapy: what, where, why, and how. Photochem. Photobiol. Sci. 1: 1–21
13. Agarwal ML, Larkin HE, Zaidi SIA, Mukhtar H and Oleinick NL (1993) Phospholipase activation triggers apoptosis in photosensitized mouse lymphoma cells. Cancer Res. 53: 5897–5902
14. Gupta S, Ahmad N and Mukhtar H (1998) Involvement of nitric oxide during phthalocyanine (Pc4) photodynamic therapy-mediated apoptosis. Cancer Res. 58: 1785–1788
15. Granville DJ, Carthy CM, Jiang H, Levy JG, McManus BM, Matroule JY, Piette J and Hunt DW (2000) Nuclear factor-kappaB activation by the photochemotherapeutic agent verteporfin. Blood 95: 256–262
16. Luna MC, Wong S and Gomer CY (1994) Photodynamic therapy-mediated oxidative stress as a molecular switch for the temporal expression of genes ligated to the human heat shock promoter. Cancer Res. 54: 1374–1380
17. Gomer CJ, Ryter SW, Ferrario A, Rucker N, Wong S and Fisher AMR (1996) Photodynamic therapy-mediated oxidative stress can induce expression of heat shock proteins. Cancer Res. 56: 2355–2360
18. Beal FM (2002) Oxidatively modified proteins in aging and disease. Free Radic. Biol. Med. 32: 797–803
19. Cabiscol E, Piulats E, Echave P, Herrero E and Ros J (2000) Oxidative stress promotes specific protein damage in *Saccharomyces cerevisiae*. J. Biol. Chem. 275: 27393–27398
20. Tamarit J, Cabiscol E and Ros J (1998) Identification of the major oxidatively damaged proteins in *Escherichia coli* cells exposed to oxidative stress. J. Biol. Chem. 273: 3027–3032
21. Das N, Levine RL, Orr WC and Sohal RS (2001) Selectivity of protein oxidative damage during aging in *Drosophila melanogaster*. Biochem. J. 360 (Part 1): 209–216
22. Choi J, Conrad CC, Dai R, Malakowsky CA, Talent JM, Carroll CA, Weintraub ST and Gracy RW (2003) Vitamin E prevents oxidation of antiapoptotic proteins in neuronal cells. Proteomics 3: 73–77
23. Stadtman ER and Levine RL (2000) Protein oxidation. Ann. NY Acad. Sci. 899: 191–208
24. Reinheckel T, Korn S, Mohring S, Augustin W, Halangk W and Shild L (2000) Adaptation of protein carbonyl detection to the requirements of proteome analysis demonstrated for hypoxia/reoxygenation in isolated rat liver mitochondria. Arch. Biochem. Biophys. 376: 59–65
25. Ettorre A, Andreassi M, Anselmi C, Neri P, Andreassi L and Di Stefano A (2003) Involvement of oxidative stress in apoptosis induced by a mixture of isothiazolinones in normal human keratinocytes. J. Invest. Dermatol. 121: 328–336
26. Hall AG (1999) The role of glutathione in the regulation of apoptosis. Eur. J. Clin. Invest. 29: 238–245
27. Slater AFG, Stefan C, Nobel I, van der Dobbelsteen DJ and Orrenius S (1996) Intracellular redox changes during apoptosis. Death Differ. 3: 57–62
28. Meister A (1995) Mitochondrial changes associated with glutathione deficiency. Biochim. Biophys. Acta 1271: 35–42
29. Morgan J and Oseroff AR (2001) Mitochondria-based photodynamic anti-cancer therapy. Adv. Drug Deliv. Rev. 49: 71–86
30. Ettorre A, Soldani P, Fabbrini M, Neri P and Di Stefano A (2002) ROS production and alteration of mitochondrial transmembrane potential after PDT with Purpurin-18 in human leukemia cells. Int. J. Biochem. 51: 86
31. Gieffers C, Korioth F, Heimann P, Ungermann C and Frey J (1997) Mitofilin is a transmembrane protein of the inner mitochondrial membrane expressed as two isoforms. Exp. Cell Res. 232: 395–399
32. Odgren PR, Toukatly G, Bangs PL, Gilmore R and Fey EG (1996) Molecular characterization of mitofilin (HMP), a mitochondria-associated protein with predicted coiled coil and intermembrane space targeting domains. J. Cell Sci. 109 (Part 9): 2253–2264
33. Gerner C, Fröhwein U, Gotzmann J, Bayer E, Gelbmann D, Bursch W and Schulte-Hermann R (2000) The Fas-induced apoptosis analyzed by high throughput proteome analysis. J. Biol. Chem. 275: 39018–39026
34. Grebenova D, Halada P, Stulik J, Havlicek V and Hrkal Z (2000) Protein changes in HL60 leukemia cells associated with 5-aminolevulinic acid-based

photodynamic therapy. Early effects on endoplasmic reticulum chaperones. Photochem. Photobiol. 72: 16–22
35. Raggiaschi R, Cocchi A, Liberatori S, Armini A, Fantetti L, Bini L and Roncucci G (2002) Analysis of the *Candida albicans* protein pattern in response to the photodynamic therapy by two-dimensional gel electrophoresis and mass-spectrometry. From Genome to Proteome: functional proteomics, fifth Siena Meeting Sept 2–5, Siena Italy pp 351
36. Berlett BS and Stadtman ER (1997) Protein oxidation in aging, disease and oxidative stress. J. Biol. Chem. 272: 20313–20316
37. Finkel T and Holbrook NJ (2000) Oxidants, oxidative stress and the biology of ageing. Nature 408: 239–247
38. Aksenov MY, Arsenova MV, Butterfield DA, Geddes JW and Markesbery WR (2001) Protein oxidation in the brain of Alzheimer's disease. Neuroscience 103: 373–383
39. Alam ZI, Daniel SE, Lees AJ, Mardsen DC, Jenner P and Halliwell BA (1997) A generalised increase in protein carbonyls in the brain in Parkinson's but incidental lewy body disease. J. Neurochem. 69: 1326–1329
40. Hartl FU (1996) Molecular chaperones in cellular protein folding. Nature 381: 571–579
41. Moser DD, Caron AW, Bourget L, Denis-Larose C and Massie B (2000) Role of the human heat shock protein hsp70 in protection against stress-induced apoptosis. Mol. Cell. Biol. 17: 5317–5327
42. Lin KM, Lin B, Lian IY, Mestril R, Scheffler IE and Dillmann WH (2001) Combined and individual mitochondrial HSP60 and HSP10 expression in cardiac myocytes protects mitochondrial function and prevents apoptotic cell deaths induced by simulated ischemia-reoxygenation. Circulation 103: 1787–1792
43. Michalak M, Corbett EF, Mesaeli N, Nakamura K and Opas M (1999) Calreticulin: one protein, one gene, many functions. Biochem. J. 344 (Part 2): 281–292
44. Gurbuxani S, Schmitt E, Cande C, Parcellier A, Hammann A, Daugas E, Kouranti I, Spahr C, Pance A, Kroemer G and Garrido C (2003) Heat shock protein 70 binding inhibits the nuclear import of apoptosis-inducing factor. Oncogene 22: 6669–6678
45. Garrido C, Schmitt E, Cand C, Vahsen N, Parcellier A and Kroemer G (2003) HSP27 and HSP70: potentially oncogenic apoptosis inhibitors. Cell Cycle 2: 579–584
46. Rabek JP, Boylston III WH and Papaconstantinou J (2003) Carbonylation of ER chaperone proteins in aged mouse liver. Biochem. Biophys. Res. Commun. 305: 566–572
47. Castegna A, Aksenov M, Thongboonkerd V, Klein JB, Pierce WM, Booze R, Markesbery WR and Butterfield DA (2002) Proteomic identification of oxidatively modified proteins in Alzheimer's disease brain. Part II: dihydropyrimidinase-related protein 2, α-enolase and heat shock cognate 71. J. Neurochem. 82: 1524–1532
48. Liu H, Miller E, van de Water B and Stevens JL (1998) Endoplasmic reticulum stress proteins block oxidant-induced Ca^{2+} increases and cell death. J. Biol. Chem. 273: 12858–12862
49. Schüler H, Nyakern M, Schutt CE, Lindberg U and Karlssoon R (2000) Mutational analysis of arginine 177 in the nucleotide binding site of beta-actin. Eur. J. Biochem. 267: 4054–4062
50. Chen Q, Chai Y-C, Mazumder S, Jiang C, Macklis RM, Chisolm GM and Almasan A (2003) The late increase in intracellular free radical oxygen species during apoptosis is associated with cytochrome *c* release, caspase activation, and mitochondrial dysfunction. Cell Death Differ. 10: 323–334
51. Treumer J and Valet G (1986) Flow-cytometric determination of glutathione alterations in vital cells by *o*-phthaldialdehyde (OPT) staining. Exp. Cell Res. 163: 518–524
52. Bradford MM (1976) A rapid and sensitive method for the quantitation of microgram quantities of protein utilizing the principle of protein-dye binding. Anal. Biochem. 72: 248–254
53. Bjellqvist B, Pasquali C, Ravier F, Sanchez JC and Hochstrasser DF (1993) A nonlinear wide-range immobilized pH gradient for two-dimensional electrophoresis and its definition in a relevant pH scale. Electrophoresis 14: 1357–1365
54. Gorg A, Postel W and Gunther S (1988) The current state of two-dimensional electrophoresis with immobilized pH gradients. Electrophoresis 9: 531–546
55. Hochstrasser DF, Harrington MG, Hochstrasser AC, Miller MJ and Merril RC (1988) Methods for increasing the resolution of two-dimensional protein electrophoresis. Anal. Biochem. 173: 424–435
56. Oakley BR, Kirsch DR and Morris R (1981) A simplified ultrasensitive silver stain for detecting proteins in polyacrylamide gels. Anal. Biochem. 106: 361–363
57. Towbin H, Staehlin T and Gordon J (1979) Electrophoretic transfer of proteins from polyacrylamide gels to nitrocellulose sheets: procedure and some applications. Proc. Natl. Acad. Sci. USA 76: 4350–4354
58. Magi B, Bini L, Marzocchi B, Liberatori S, Raggiaschi R and Pallini V (1999) Immunoaffinity identification of 2-DE separated proteins. Methods Mol. Biol. 112: 431–443
59. Hellman U, Wernstedt C, Gonez J and Heldin CH (1995) Improvement of an 'In-Gel' digestion procedure for the micropreparation of internal protein fragments for amino acid sequencing. Anal. Biochem. 224: 451–455
60. Soskic V, Gorlach M, Poznanovic S, Boehmer FD and Godovac-Zimmermann J (1999) Functional proteomics analysis of signal transduction pathways of the platelet-derived growth factor beta receptor. Biochemistry 38: 1757–1764